

# Impurity induced spin gap asymmetry in nanoscale graphene

Julia Berashevich and Tapash Chakraborty\*

*Department of Physics and Astronomy, University of Manitoba, Winnipeg, Canada, R3T 2N2*

We propose a unique way to control both bandgap and the magnetic properties of nanoscale graphene, which might prove highly beneficial for application in nanoelectronic and spintronic devices. We have shown that chemical doping by nitrogen along a single zigzag edge breaks the sublattice symmetry of graphene. This leads to the opening of a gap and a shift of the molecular orbitals localized on the doped edge in such a way that the spin gap asymmetry, which can lead to half-metallicity under certain conditions, is obtained. The spin-selective behavior of graphene and tunable spin gaps help us to obtain semiconductor diode-like current-voltage characteristics, where the current flowing in one direction is preferred over the other. The doping in the middle of the graphene layer results in an impurity level between the HOMO and LUMO orbitals of pure graphene (again, much like in semiconductor systems) localized on the zigzag edges thus decreasing the bandgap and adding unpaired electrons, and this can also be used to control graphene conductivity.

## I. INTRODUCTION

Applications of graphene with its unique physical properties<sup>1,2,3,4,5</sup> in nanoelectronics<sup>6,7</sup>, magnetism and spintronics<sup>8,9,10,11,12</sup>, hang crucially on its bandgap and spin ordering at the zigzag edges. A bandgap can be opened in graphene by breaking the certain symmetries. For example, interaction of graphene with its substrate, such as SiC, leads to the charge exchange between them which breaks the sublattice symmetry<sup>13</sup>. Moreover, the quantum confinement effect also has been found to introduce a small bandgap in graphene nanoribbons<sup>14</sup>, just as was predicted earlier theoretically<sup>15,16,17,18</sup>. The effect of bandgap opening and spin ordering between the zigzag edges are found to be directly linked to each other<sup>20</sup>. When the spins align along the zigzag edges and spin states localized at opposite edges have the same spin orientation, then symmetry of graphene is preserved and the system is gapless. Otherwise, if the spin-up states are localized along one zigzag edge and the spin-down along the other, the sublattice symmetry is broken which leads to a gap. In the light of a recent breakthrough in fabrication of nanoribbons of required size through unzipping of carbon nanotubes, the nanoribbons and nanoscale graphene are the most promising systems for application in nanoelectronics<sup>19</sup>.

Manipulation of the spin ordering is important for both graphene magnetism and its electronic properties. There are several approaches which have been proposed recently to control the spin ordering along the edges<sup>21,22,23,24,25,26,27</sup>. One of them is the termination of the zigzag edges by functional groups<sup>21</sup>. This has the advantage that one can achieve half metallicity in this process. However, there are some serious issues involved here. Firstly, many of these functional groups are placed out of the graphene plane thus making the whole structure non-planar and, most importantly, termination was applied to every second edge cell, which makes its technological application very difficult. In fact, we found that the strong interactions of the graphene lattice with some

of the functional groups, such as  $\text{NH}_2$  and  $\text{NO}_2$ , lead to buckling of the graphene layer and twisting of the functional groups, which subsequently may result in the disappearance of the half-metallicity of graphene. The curling of the graphene layer has been seen in earlier studies as well<sup>27</sup>, where the boundary conditions were found to control the graphene planarity, namely the curling occurs for stand-alone systems. For nanoscale graphene the ferromagnetic ordering of the spin states along the zigzag edges can be also achieved as subsequence of adsorption of gas and water molecules on the graphene surface, as we have shown in our previous study<sup>22</sup>. The adsorption leads to pushing of the  $\alpha$ - and  $\beta$ -spin states to the opposite zigzag edges thereby breaking sublattice symmetry and opening a gap. In some cases the spin asymmetry can occur. For example, the adsorption of HF gas molecule provide the HOMO-LUMO gap of 2.1 eV for  $\alpha$ -spin state and of 1.2 eV for  $\beta$ -spin state. However, due to the weak interaction between adsorbant and graphene surface the phenomena of the spin alignment along the edges takes place locally, thus limiting its application.

The connection of the phenomena of bandgap opening and of the spin ordering with the sublattice symmetry lead us to conclude that breaking of this symmetry is the main direction to achieve the required semiconductor-type bandgap in graphene and a tunable spin ordering. Here we make a proposal that the symmetry breaking can be done by chemical doping along a single zigzag edge. This method is far superior to the earlier approaches involving edge termination by functional groups because doping can be done for every unit cell along the zigzag edge and thus preserve the planarity of graphene. Doping not only breaks the graphene symmetry, but also can induce the spin gap asymmetry due to the energetic shift of the molecular orbitals localized on the doped edge. In a structure with broken symmetry, the  $\text{HOMO}_\alpha$  and  $\text{LUMO}_\beta$  orbital states are localized at one edge, while  $\text{HOMO}_\beta$  and  $\text{LUMO}_\alpha$  are at the other. Suppose the doping shifts the  $\text{HOMO}_\alpha$  and  $\text{LUMO}_\beta$  orbital states localized at one edge down, then the  $\text{HOMO}_\alpha$ - $\text{LUMO}_\alpha$  bandgap ( $\Delta_\alpha$ ) is increased, while  $\Delta_\beta$ , in contrast, will

be reduced. If a certain type of impurities can cause a significant shift of the bands, then the half-metallicity of graphene may occur. This is what we set out to investigate here. An important advantage of this approach is that we expect insensitivity of spin selective behavior to the quality of the edges, when the band shift induced by the impurities is stronger than the contribution from the edge defects. We also investigate the possibility of obtaining an impurity level in the middle of the graphene bandgap by doping (in analogy to semiconductors), which has a lot of technological implications as well. Our study of nanoscale graphene was based on the quantum chemistry methods using the spin-polarized density functional theory with the semilocal gradient corrected functional (UB3LYP/6-31G) performed in the Jaguar 7.5 program<sup>28</sup>.

## II. SYMMETRY OF NANOSCALE GRAPHENE

Bulk graphene has hexagonal symmetry, while the highest possible symmetry of nanoscale graphene would be the D2h planar symmetry with an inversion center. The D2h symmetry results in structurally identical corners exhibiting ferromagnetic ordering of the spin-polarized states localized at the corners, as presented in Fig. 1 (a). According to the NBO (natural bond orbital) analysis, the localized electrons at the corners are unpaired *sp* electrons belonging to non-bonded orbitals, which are located at the bottom of conduction band or top of the valence band. For this symmetry, both  $\alpha$ - and  $\beta$ -spin states of the HOMO and LUMO orbitals are localized on the zigzag edges but their spin density is equally distributed between two edges. For nanoscale graphene of D2h symmetry the HOMO-LUMO gap appears due to confinement and edge effects<sup>15</sup>. The degeneracy of the  $\alpha$ - and  $\beta$ -spin states belonging to the HOMO and LUMO orbitals depends on the edge configuration, i.e.,  $\alpha$ - and  $\beta$  states can be non-degenerate or degenerate depending on number of the carbon rings along the zigzag and armchair edges<sup>22</sup>. The degeneracy reappears for large structures, such as  $n \geq 8$ ,  $m \geq 7$  (see notation in Fig. 1 (a)). The increase of the graphene size leads to disappearance of the confinement effect and as a result closing of the gap. Thus, for  $n = 4$  and  $m = 5$  the gap is  $\sim 0.5$  eV and already for  $n = 6$  and  $m = 7$  the gap is suppressed to  $\sim 0.19$  eV. The influence of the confinement effect on the graphene gap has been already confirmed experimentally<sup>14</sup>.

However, the state of D2h symmetry is not the ground state for nanoscale graphene. Graphene, optimized with C2v symmetry, where the mirror plane of symmetry is parallel to the armchair edges, has a total energy lower than that for the D2h symmetry. For the C2v symmetry, the HOMO and LUMO orbitals are characterized by the  $\alpha$ - and  $\beta$ -spin states localized on the opposite zigzag edges. Because the carbon atoms at the opposite zigzag edges belong to different sublattices, such spin distribu-

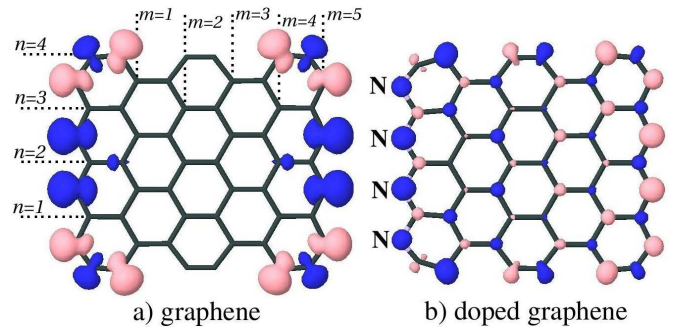


FIG. 1: (color online). The spin density distribution: (a) for nanoscale graphene optimized with the D2h point-group symmetry, and (b) for the case when one edge is doped by nitrogen, where the highest symmetry is the planar symmetry. Different colors indicate the  $\alpha$ - (light) and  $\beta$ -spin (dark) states. The spin density is plotted for isovalues of  $\pm 0.01$  e/ $\text{\AA}^3$ . The  $n$  and  $m$  are introduced to identify the number of the carbon rings along the zigzag edge ( $n$ ) and along the armchair edge ( $m$ ).

tion breaks sublattice symmetry and opens a gap ( $\sim 1.63$  eV for  $n = 4$  and  $m = 5$ ). The size of the gap is comparable to that found for nanoribbons<sup>20</sup>. The large gap of nanoscale graphene obtained here is a result of significant contribution of the confinement effect, as the nanoscale graphene is confined in all directions.

The localization of the  $\alpha$ - and  $\beta$ -spin states belonging to HOMO and LUMO at the opposite zigzag edges is important for the application of graphene in spintronics<sup>8,9,29,30</sup>. However, the C2v symmetry state is a highly metastable state. Its total energy is comparable to that of D2h symmetry with a difference of  $\sim -0.5$  eV for small structures such as  $n = 4$  and  $m = 5$ , but the difference decreases exponentially down to  $\sim -0.02$  eV with increasing the structure size up to  $n \geq 6$  and  $m \geq 7$ , that has good agreement with earlier work<sup>17</sup>, and disappears when  $n > 8$  and  $m > 8$ . The competition of the C2v state with C1 symmetry, which is not constrained to have spin ordering along the zigzag edge, is even more crucial because of almost identical magnitude of their total energy. However, we found that the distortion or dissimilarity induced along a single zigzag edge not only breaks the sublattice symmetry of the graphene, but can control the spin ordering, thereby stabilizing the ground state of the C2v symmetry. The highest possible symmetry of the doped graphene is lowered from D2h to C2v symmetry as a result of the edge dissimilarity. The spin density distribution for the nanoscale graphene with one zigzag edge doped by nitrogen is presented in Fig. 1 (b). The localized states along the zigzag edges are formed by unpaired electrons belonging to the natural non-bonded orbitals, which participate in formation of HOMO and LUMO orbitals. The  $\alpha$ - and  $\beta$ -spin states of HOMO and LUMO orbitals are spatially separated, i.e. localized at opposite zigzag edges. The (HOMO-1) and (LUMO+1) orbitals usually correspond to the surface states, redistributed

over the entire graphene structure. The surface states are important for conductivity of graphene in a transverse electric field, because the charge transfer between the spatially separated HOMO and LUMO orbitals may occur through participation of the surface states. The electron density distribution for the edge states and the surface states is presented in Fig. 2. The slight difference between the  $\alpha$ - and  $\beta$ -spin surface states (HOMO-1) is due to doping of the left zigzag edge. The  $\alpha$ - and  $\beta$ -spin states remain spatially separated with increasing structure size.

### III. HALF-METALLICITY OF GRAPHENE

The edge dissimilarity allows us to explore the required properties, such as the semiconductor-type bandgap and localization of  $\alpha$ - and  $\beta$ -spin states at opposite zigzag edges. Moreover, the spatial separation of the  $\alpha$ - and  $\beta$ -spin states resulted from doping of the single zigzag edge is stable in comparison to the water adsorption<sup>22</sup>. Doping of a single edge shifts the band energies of the orbitals which are strongly localized at this edge. Such a shift provides an opportunity to obtain another useful property which is important for spintronics – the half-metallicity of graphene. For the HOMO or LUMO orbitals, which are shown to be localized at the edges, doping can create a strong non-degeneracy of the  $\alpha$ - and  $\beta$ -spin states, because these states are spatially separated and localized at the opposite edges. Moreover, the  $\text{HOMO}_\alpha$  and  $\text{LUMO}_\beta$  orbitals are localized at one edge, while  $\text{HOMO}_\beta$  and  $\text{LUMO}_\alpha$  at the other. If doping increases the bandgap  $\Delta_\alpha$  for the  $\alpha$ -spin state, then the bandgap  $\Delta_\beta$  for the  $\beta$ -spin state, in contrast will be reduced, and vice versa. Therefore, doping induces the spin gap asymmetry in graphene. Materials exhibiting asymmetric gaps for the  $\alpha$ - and  $\beta$ -spin states where one gap is of semiconductor type while the other is an insulator, are known as half-semiconductor materials, but if one of them is metallic, the system is half-metallic. Therefore, by choosing the right doping we can achieve a stable half-metallicity in graphene which will be an important step forward for applications in spintronics.

We have investigated the transformation of the electronic structure of nanoscale graphene due to the induced edge dissimilarities. The results are schematically presented in Fig. 3. For nanoscale graphene with the D2h symmetry, a small bandgap occurs due to the confinement effect. The HOMO and LUMO orbitals in this case are localized at the zigzag edges, but their electron density is equally redistributed over both edges (see Fig. 3 (a)). Termination of the left zigzag edge by hydrogen (see Fig. 3 (b)) opens a gap as a result of breaking of the sublattice symmetry, thereby lowering D2h symmetry to a stable ground state of C2v symmetry. The hydrogenation leads to saturation of the dangling  $\sigma$  bonds at the terminated edge but does not significantly change the energy of the  $\text{HOMO}_\alpha$  and  $\text{LUMO}_\beta$  states localized at

this edge. The resulting non-degeneracy of the  $\alpha$ - and  $\beta$ -spin states is not large, and the HOMO-LUMO gap of the  $\alpha$ -spin state ( $\Delta_\alpha = 1.8$  eV) is almost identical to that of the  $\beta$ -spin state ( $\Delta_\beta = 2.1$  eV). The doping of the left zigzag edge by nitrogen (see Fig. 3 (c)) shifts down the orbital energies of the  $\text{HOMO}_\alpha$  and  $\text{LUMO}_\beta$  states localized at the doped edge and results in a strong non-degeneracy of the orbitals. This leads to a slight enhancement of the HOMO-LUMO gap for the  $\alpha$ -spin state up to  $\Delta_\alpha = 2.2$  eV, but significantly decreases the HOMO-LUMO gap for the  $\beta$ -spin state down to  $\Delta_\beta = 0.8$  eV. The length of the nitrogen-carbon bond at the edges is found to be  $d_{N-C} = 1.35$  Å, which is similar to the carbon-carbon bonds  $d_{C-C} = 1.39$  Å. Similar results are obtained for phosphorus impurities, where the gaps are  $\Delta_\alpha = 2.0$  eV and  $\Delta_\beta = 0.9$  eV. Phosphorus is, however, less useful because of the large phosphorus-carbon bond ( $d_{P-C} = 1.78$  Å) which can lead to destruction of the lattice. We have also investigated the possibility to dope the single zigzag edge of the nanoscale graphene by other impurities, such as oxygen and boron, but they are not as effective as nitrogen. The oxygen doping leads to strong delocalization of the electron density of the orbitals localized at the edges. The doping by boron leads to even more troubles due to the long boron-carbon bonds at the edges ( $d_{B-C} = 1.42$  Å) and shifting of the states localized at the edges from the HOMO-LUMO gap deeper into the conduction and valence bands.

For the nanoscale graphene structure investigated in this work, the spin asymmetry is achieved but bandgap magnitude for  $\alpha$ - and  $\beta$ -spin states corresponds to the half-semiconductor behavior ( $\Delta_\alpha = 2.2$  eV,  $\Delta_\beta = 0.8$  eV). Increasing the size of the graphene results in a decrease of both the  $\Delta_\alpha$  and  $\Delta_\beta$  gaps due to the diminishing of the confinement effect. Therefore, for graphene structures doped by nitrogen or phosphorus of size  $n \geq 6$  and  $m \geq 7$ , the  $\Delta_\beta$  gap is closer to metallic type. Thus, for  $n = 6$  and  $m = 7$  the gap for  $\alpha$ -spin state is suppressed down to 1.13 eV while for  $\beta$ -spin state down to 0.19 eV, which corresponds to the *half-metallic behavior of graphene*. An external electric field applied between the zigzag edges has been shown<sup>8,9,29,30</sup> to shift the band of graphene with spatially separated and degenerated  $\alpha$ - and  $\beta$ -spin states. The electric field shifts the bands in such a way that for the  $\alpha$ -spin the HOMO and LUMO levels move closer to each other in the energy scale, while for  $\beta$ -spin they move apart. At a certain electric field  $\Delta_\alpha$  vanishes, thereby creating a metallic behavior of graphene. If  $+E_c$  electric field can close the bandgap for the  $\alpha$ -spin state, the  $-E_c$  leads to bandgap disappearance for the  $\beta$ -spin state. Therefore, the current voltage characteristic of such a structure will be symmetrical because the  $\Delta_\alpha$  equals  $\Delta_\beta$  and for both spin states the switch from the semiconductor behavior to metallic occurs at the same critical electric field  $\pm E_c$ . The advantage of graphene with spin gap asymmetry, i.e. different  $\Delta_\alpha$  and  $\Delta_\beta$  gaps, found in this work is the different values of the critical electric field required to close these gaps, such that

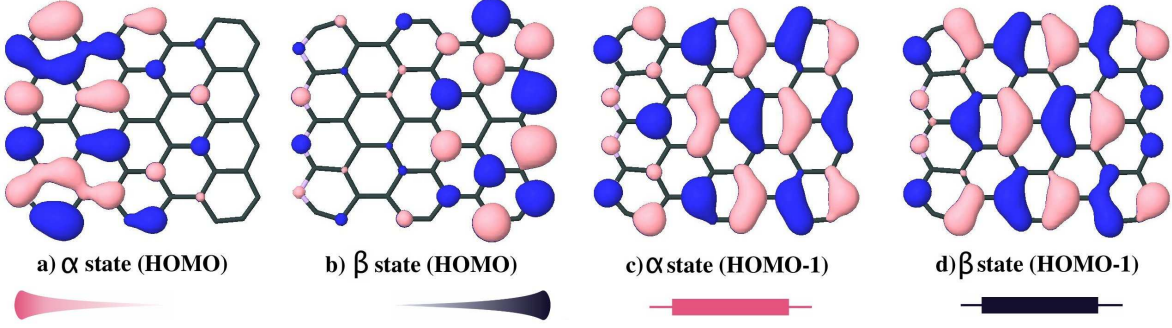


FIG. 2: (color online). Spin polarizations in nanoscale graphene where the left edge is doped by nitrogen. Different colors correspond to different signs of the molecular orbital lobes. The electron densities are plotted for isovalues of  $\pm 0.02 \text{ e}/\text{\AA}^3$ : (a)  $\alpha$ -state of HOMO ( $E_{\text{HOMO}} = -6.04 \text{ eV}$ ) (b)  $\beta$ -state of HOMO ( $E_{\text{HOMO}} = -5.43 \text{ eV}$ ) (c)  $\alpha$ -state of (HOMO-1) ( $E_{\text{HOMO}-1} = -6.38 \text{ eV}$ ) (d)  $\beta$ -state of (HOMO-1) ( $E_{\text{HOMO}-1} = -6.43 \text{ eV}$ ). The HOMO and LUMO are found to be localized at the single zigzag edges (edge states), while (HOMO-1) and (LUMO+1) – delocalized over the entire graphene structure (surface states). Bottom pictures show the representation of the localized and surface states.

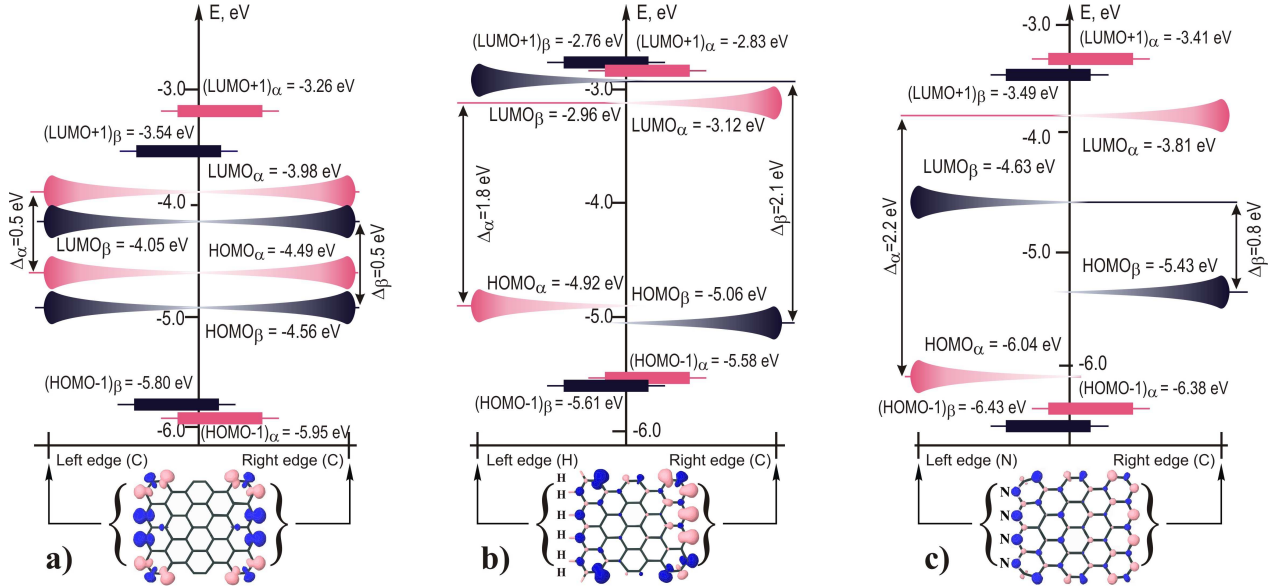


FIG. 3: (color online). Schematic diagrams showing the distribution of the edge states and surface states in the energy scale and over the graphene structure (see the bottom pictures in Fig. 2 for pictorial description of the states). The structures at the bottom demonstrate the spin distribution with isovalues of  $\pm 0.01 \text{ e}/\text{\AA}^3$ . (a) nanoscale graphene optimized with the D2h symmetry, (b) with left edge terminated by hydrogen and (c) with the left zigzag edge doped by nitrogen. For the localized states the energy levels (HOMO and LUMO) show density distribution (schematic), particularly delocalization of the orbitals between the two edges if the D2h symmetry is preserved, and their localization on the zigzag edges when sublattice symmetry is broken and C2v symmetry becomes to be highest possible symmetry. The surface states ((HOMO-1) and (LUMO+1)) are delocalized over the entire graphene structure (see for example Fig. 2 (c,d)).

$|E_{c(\beta)}| < |E_{c(\alpha)}|$  when  $\Delta_\beta < \Delta_\alpha$ . Therefore, this structure will be characterized by the spin-polarized current and by a non-symmetric current-voltage characteristics as for a semiconductor diode, when the current flow in one direction is preferable to the other.

#### IV. DOPING OF GRAPHENE

We have also investigated the influence of impurities on the electronic structure of graphene in the case when they are not embedded at the zigzag edges. Replacing carbon atoms by nitrogen atoms in a graphene lattice results in the appearance of impurity levels *inside* of both the  $\Delta_\alpha$  and  $\Delta_\beta$  gaps. The energy diagram of localization of the molecular orbitals for the doped graphene is presented in Fig. 4. As we mentioned earlier, in pure

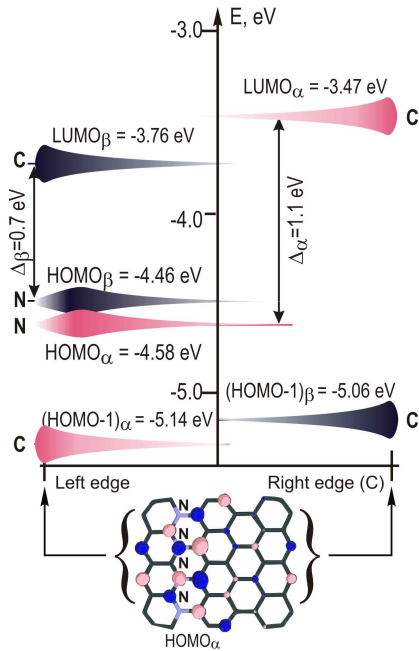


FIG. 4: (color online). Schematic diagram showing the distribution of the edge states (LUMO, HOMO-1) and states localized by the dopant in the middle of the graphene structure (HOMO) (see the bottom pictures in Fig. 2 for pictorial description of the states). The  $\text{HOMO}_\alpha$  and  $\text{HOMO}_\beta$  are extra impurity levels that appear due to the doping and replaces the occupied orbital localized on the left carbon edge by shifting it deeper into the valence band. The inset picture (in brackets) demonstrates the electron density distribution for the  $\text{HOMO}_\alpha$  with isovalues of  $\pm 0.01 \text{ e}/\text{\AA}^3$ .

graphene the HOMO and LUMO orbitals are localized at the zigzag edges. The applied doping creates one extra occupied orbital (HOMO) which is localized at the embedded nitrogen atoms and located above the occupied orbital belonging to edges, which becomes HOMO-1. The NBO analysis has shown that this extra orbital is formed by the unpaired  $sp$  electron localized on each nitrogen atoms. This reduces the HOMO-LUMO gap ( $\Delta_\alpha = 1.1 \text{ eV}$  and  $\Delta_\beta = 0.7 \text{ eV}$ ) while preserving the spin asymmetry.

In an applied in-plane electric field the charge transfer occurs between the orbitals localized on the opposite zigzag edges, i.e., in our case such transfer occurs between the HOMO-1 and LUMO orbitals, which is a multi-step process with participation of HOMO. Because the gap is decreased and each nitrogen atom adds an unpaired electron into the system due to the doping, the conductivity of graphene would be significantly enhanced, and can be controlled as it is done in semiconductor devices.

## V. CONCLUSION

We have investigated the possibility to control the electronic and magnetic properties of nanoscale graphene. We found that if pure graphene can be characterized by a small bandgap and no spin ordering at the zigzag edges the dissimilarity of the edges induced by doping impurities lowers the highest possible symmetry to  $C_{2v}$ , which is characterized by the spin ordering along the zigzag edges and their antiparallel alignment between opposite zigzag edges. Moreover, impurities embedded at a single zigzag edge shifts in the energy scale the molecular orbitals localized at this edge, thereby decreasing the bandgap for one spin channel and increasing the other. Under these conditions, the half-metallic behavior can be achieved. Nitrogen doping in the middle of the graphene surface is found to have the prospect for application in nanoelectronics due to the appearance of the occupied impurity levels in the bandgap. The impurity level results in a decrease of the bandgap of  $\sim 2.0 \text{ eV}$  by one half and contains unpaired electrons, which should lead to an enhancement of the conductivity. Therefore, both the conductivity of the nanoscale graphene and its magnetic properties can be controlled by the impurities.

## VI. ACKNOWLEDGMENTS

The work was supported by the Canada Research Chairs Program and the NSERC Discovery Grant.

\* Electronic address: chakrabort@cc.umanitoba.ca

<sup>1</sup> A.K. Geim and K.S. Novoselov, *Nature Materials* **6**, 183 (2007).

<sup>2</sup> Y. Zhang, Y.-W. Tan, H.L. Stormer, and P. Kim, *Nature* **438**, 201 (2005).

<sup>3</sup> V.M. Apalkov and T. Chakraborty, *Phys. Rev. Lett.* **97**, 126801 (2006).

<sup>4</sup> X.-F. Wang and T. Chakraborty, *Phys. Rev. B* **75**, 041404 (2007).

<sup>5</sup> D.S.L. Abergel and T. Chakraborty, *Phys. Rev. Lett.* **102**, 056807 (2009).

<sup>6</sup> Z. Chen, Y.-M. Lin, M.J. Rooks, and P. Avouris, *Physica E* **40**, 228 (2007).

<sup>7</sup> E.J.H. Lee, K. Balasubramanian, R. T. Weitz and M. Burghard, *Nature Nanotechnology* **3**, 486 (2008).

<sup>8</sup> Y.-W. Son, M. L. Cohen and S.G. Louie, *Nature* **444**, 347 (2006).

<sup>9</sup> E. Rudberg, P. Salek, and Y. Luo, *Nano Letters* **7**, 2211 (2007).

<sup>10</sup> P. Esquinazi, D. Spemann, R. Hühne, A. Setzer, K.-H. Han and T. Butz, *Phys. Rev. Lett.* **91**, 227201 (2003).

<sup>11</sup> S. Cho, Y. Chen, and M.S. Fuhrer, *Appl. Phys. Lett.* **91**, 123105 (2007).

<sup>12</sup> V.M. Kapran, G. Giovannetti, P.A. Khomyakov, M. Talanana, A.A. Starikov, M. Zwierzycki, J. van der Brink, G. Brocks and P.J. Kelly, *Phys. Rev. Lett.* **99**, 176602 (2007).

- <sup>13</sup> S.Y. Zhou, D.A. Siegel, A.V. Fedorov and A. Lanzara, Phys. Rev. Lett. **101**, 086402 (2008).
- <sup>14</sup> M.Y. Han, B. Özyilmaz, Y. Zhang and P. Kim, Phys. Rev. Lett **98**, 206805 (2007).
- <sup>15</sup> Y.-W. Son, M. L. Cohen and S.G. Louie, Phys. Rev. Lett. **97**, 216803 (2006).
- <sup>16</sup> K. Nakada, M. Fujita, G. Dresselhaus and M.S. Dresselhaus, Phys. Rev. B **54**, 17954 (1996).
- <sup>17</sup> H. Lee, Y.-W. Son, N. Park, S. Han and J. Yu, Phys. Rev. B **72**, 174431(2005).
- <sup>18</sup> L. Pisani, B. Montanari and N.M. Harrison, New Journal of Physics **10**, 033002 (2008).
- <sup>19</sup> D. V. Kosynkin, A. Higginbotham, A. Sinitskii, J. R. Lomeda, A. Dimiev, B. K. Price and J. Tour, Nature **458**, 872 (2009); L. Jiao, L. Zhang, X. Wang, G. Diankov and H. Dai, Nature **458**, 877 (2009).
- <sup>20</sup> L. Pisani, J.A. Chan, B. Montanari and N.M. Harrison, Phys. Rev. B **75**, 064418 (2007).
- <sup>21</sup> F. Cervantes-Sodi, G. Csányi, S. Piscanec, and A.C. Ferrari, Phys. Rev. B **77**, 165427 (2008).
- <sup>22</sup> J. Berashevich and T. Chakraborty, arXiv:0901.4956.
- <sup>23</sup> D. Gunlycke, J.Li, J.W. Mintmire and C.T. White, Appl. Phys. Lett.**91**, 112108 (2007).
- <sup>24</sup> D.W. Boukhvalov and M.I. Katsnelson, Nano Letters **8**, 4373 (2008).
- <sup>25</sup> Z. Li, J. Yang and J.G. Hou, J. Am. Chem. Soc.**130**, 4224 (2008).
- <sup>26</sup> O. Hod, V. Barone, J.E. Peralta and G.E. Scuseria, Nano Letters **7**, 2295 (2007).
- <sup>27</sup> E.-J. Kan, X. Wu, Z. Li, X.C. Zeng, J. Yang and J.G. Hou, J. Chem. Phys. **129**, 084712 (2008).
- <sup>28</sup> Jaguar, version 7.5. Schrödinger **2007**. LLC: New York, NY.
- <sup>29</sup> O. Hod, V. Barone and G. E. Scuseria, Phys. Rev. B **77**, 035411 (2008).
- <sup>30</sup> S. Dutta and S. K. Pati, J. Phys. Chem. B **112**, 1333 (2008).